Available online at www.sciencedirect.com
ScienceDirect
Trans. Nonferrous Met. Soc. China 25(2015) 1427−1438
Transactions of Nonferrous Metals Society of China
www.tnmsc.cn

Corrosion performance of friction stir welded AA2024 aluminium alloy under salt fog conditions

R. SEETHARAMAN[1], V. RAVISANKAR[1], V. BALASUBRAMANIAN[2]

1. Department of Manufacturing Engineering, Annamalai University, Annamalainagar, Chidambaram 608 002, Tamil nadu, India;
2. Center for Materials Joining & Research, Department of Manufacturing Engineering, Annamalai University, Annamalainagar, Chidambaram 608 002, Tamil nadu, India

Received 9 April 2014; accepted 14 August 2014

Abstract: Aluminium alloy (AA) 2024 is an important engineering material due to its widespread use in the aerospace industry. However, it is very prone to corrosion attack in chloride containing media. In the present investigation, AA2024 aluminium alloy rolled plates of 5 mm in thickness were friction stir welded. Corrosion performances of the specimens were evaluated by conducting salt fog tests in NaCl solution at different pH values, chloride ion concentrations and spraying time. In addition, an empirical relationship was established to predict the corrosion rate of friction stir welds of AA2024 aluminium alloy. A central composite rotatable design including three factors and five levels was used to minimize the number of experiments. Response surface methodology (RSM) was used to develop the relationship. The corrosion rate decreased under neutral pH conditions. The corrosion rate increased in acidic and basic conditions. It was also found that the corrosion rate decreased with the increase of spraying time, but the corrosion tended to be uniform with the increment of time and with the increase in the chloride ion concentration, and the corrosion rate increased in the salt spray corrosion test.

Key words: AA2024 aluminium alloy; friction stir welding; salt fog test; response surface methodology; corrosion rate

1 Introduction

High strength AA2024 aluminium alloy, as a typical precipitation hardening aluminium alloy, is difficult to join by conventional techniques, such as gas tungsten arc welding (GTAW) and gas metal arc welding (GMAW), because of hot cracking sensitivity and significant strength drop in the joint [1]. Friction stir welding (FSW), invented by the Welding Institute (TWI) in 1991 as a new solid state joining technique that can provide localized modification and control of microstructures [2], has the advantages of reducing the grain size, refining the microstructure and improving the mechanical properties compared to the conventional welding. FSW is ideal for joining aluminium alloys, especially for AA2000 and AA7000 series aluminium alloys [3−5].

In the welding field, extensive researches on friction stir welded joints for AA2000 or AA7000 series aluminium alloys have been carried out in the past decade focusing on microstructural characteristics, mechanical properties, residual stress analysis, plastic flow patterns and numerical simulation for the temperature field [6−8]. However, there are only few investigations related to the corrosion properties of the FSW aluminium alloys.

The electrochemical behaviour of aluminum and its alloys has been the subject of a large number of publications [9,10]. The corrosion of aluminum alloy friction stir welds was commonly investigated using methods such as immersion tests, polarization techniques and electrochemical impedance spectroscopy (EIS) [11,12]. Some studies have been undertaken about the effect of pH on the rate of corrosion [13,14]. The corrosion properties of various zones of FSW have been examined by a number of investigators. Corrosion attack in the nugget has been found for AA2024-T351 alloys [15]. Studies have shown attack occurring predominantly in stir zone (SZ), for example in AA2024-T351 [16].

The effect of FSW on the corrosion behaviour of AA2024-T4 and Al–Li alloys (AA2195) was investigated and showed that the diffusion-limiting

Corresponding author: R. SEETHARAMAN; Tel: +91-9442573993; E-mail: r.seetharamanme@gmail.com
DOI: 10.1016/S1003-6326(15)63742-6

current densities and corrosion potentials of both AA2024 and AA2195 FSW welds were nearly identical to those of the base alloys for a 0.6 mol/L NaCl solution.

From the literature review, it is understood that most of the published researches on friction stir welded aluminium alloys were focused on mechanical properties. Very few investigation has been done to explore the corrosion properties of friction stir welded AA2024 aluminium alloys. No investigation was carried out by incorporating the effect of pH values, chloride ion concentration and immersion time on the corrosion behaviour of friction stir welded AA2024 aluminium alloys. Hence, the present investigation was carried out to study the corrosion behaviour of AA2024 aluminium alloy welds. Furthermore, an empirical relationship was developed to predict the corrosion rate of friction stir welds of AA2024 aluminium alloy under salt fog conditions.

2 Experimental

2.1 Specimen preparation

The material used in this work was AA2024 aluminium alloy in the form of rolled plates of 5 mm thickness. The chemical composition and mechanical properties of the base metal are presented in Tables 1 and 2.

Table 1 Chemical composition of AA2024 aluminium alloy (mass fraction, %)

Mg	Mn	Fe	Si	Cu	Zn	Al
1.42	0.61	0.08	0.06	4.43	0.06	Bal.

Table 2 Mechanical properties of AA2024 aluminium alloy

Yield strength/ MPa	Ultimate tensile strength/ MPa	Elongation/ %	Vickers hardness (HV)
310	402	23	140

The optical micrograph of base metal is shown in Fig. 1. The plate was cut to a required size (300 mm× 150 mm) by power hacksaw followed by milling. The square butt joint configuration was prepared to fabricate the joints. The initial joint configuration was obtained by securing the plates in position using mechanical clamps. The direction of welding was normal to the extruded direction. Single pass welding procedure was followed to fabricate the joints. A non-consumable tool made of high carbon steel was used. An indigenously designed and developed computer numerical controlled friction stir welding (22 kW; 4000 r/min; 60 kN) was used to fabricate joints. The FSW parameters were optimized by conducting trial runs and the welding conditions which produced defect free joints were taken as optimized welding conditions. The optimized welding conditions used to fabricate the joints in this investigation are presented in Table 3.

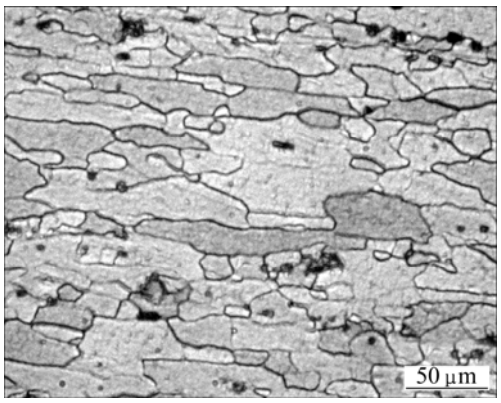

Fig. 1 Optical micrograph of AA2024 alloy

From the welded joints, the corrosion test specimens were extracted from the friction stir welds with the dimensions of 15 mm×15 mm×5 mm, as shown in Fig. 2.

The specimens were ground with 500, 800, 1200, 1500 grit SiC paper. Finally, they was cleaned with acetone and washed in distilled water and then dried by warm flowing air. The optical micrograph of the friction stir weld region is shown in Fig. 3.

2.2 Corrosion test parameters

From Refs. [17−21], the predominant factors that have a greater influence on corrosion behaviour of AA2024 aluminium alloy are identified, including pH value of the solution, corrosion time and chloride ion concentration. Large numbers of trial experiments were conducted to identify the feasible testing conditions using friction stir welded AA2024 aluminium alloy under salt fog conditions. The following inferences are obtained:

1) If pH value of the solution is less than 3, the amphoteric property of the aluminium oxide fades away. In addition, the change in chloride ion concentration does

Table 3 Optimized welding conditions and process parameters used to fabricate joints

Rotational speed/(r·min^{-1})	Welding speed/ (mm·min^{-1})	Axial force/ kN	Tool shoulder diameter/mm	Pin diameter/ mm	Pin length/ mm	Pin profile
1500	75	10	15	5	4.7	Left hand thread of 1 mm pitch

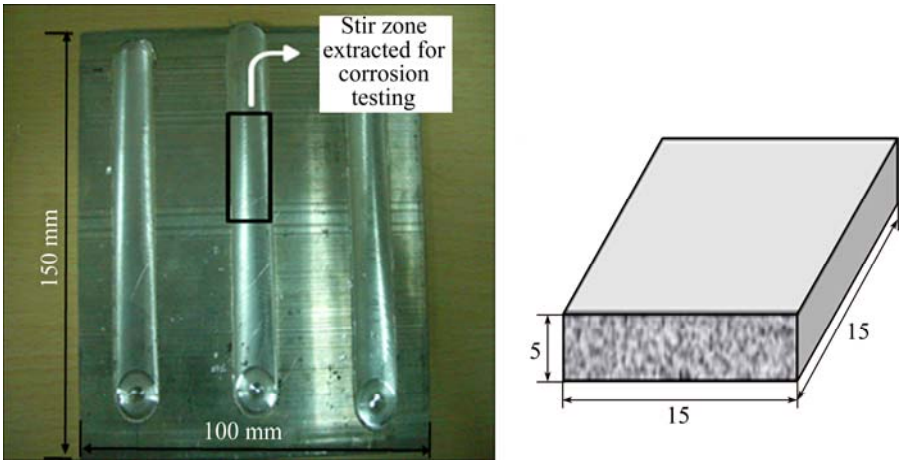

Fig. 2 Extraction and dimensions of corrosion specimen (unit: mm)

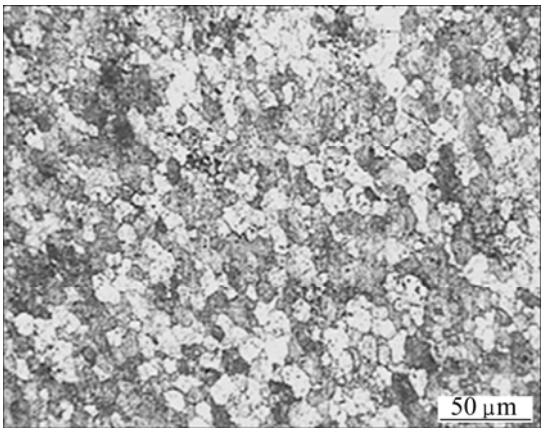

Fig. 3 Optical micrograph of friction stir welded AA2024 alloy

not considerably affect the corrosion. It shows no passivity.

2) If the pH value is between 3 and 11, the main degradation mechanism in the pH value from 3 to 11 is pitting corrosion and the pitting potential is independent over this pH range.

3) If pH value is greater than 11, i.e., spraying to very alkaline solutions, the corrosion results in relatively stable steady open circuit potential. No change has been observed in pitting potential. However, it states that aluminium is prone to more pitting in alkaline solutions close to neutrality.

4) If the chloride ion concentration is less than 0.2 mol/L, visible corrosion will not occur in the experimental period. No pitting was observed in lower concentration.

5) If the chloride ion concentration is between 0.2 mol/L and 1 mol/L, there was a reasonable fluctuation in the corrosion rate. The anodic behaviours of samples during spraying to 0.2 mol/L up to 1 mol/L NaCl solutions are similar, each exhibiting pitting potential φ_{pit} at the corrosion potential (φ_{corr}).

6) If the chloride ion concentration is greater than 1 mol/L, a rise in corrosion rate might hesitate and decrease a little.

7) If the corrosion time is less than 24 h, the surface is completely covered with the thick and rough corrosion products and has an unpredicted corrosion rate.

8) If the corrosion time is between 24 and 104 h, the tracks of the corrosion could be predicted. As per ASTM standards, for salt spraying experiment, the minimum of 48 h testing time is required.

9) If the corrosion time is greater than 104 h, the tracks of corrosion film are difficult to identify.

2.3 Developing experimental design matrix

Owing to a wide range of factors, three factors and central composite rotatable design matrix were chosen to minimize number of experiments. Design matrix consisting of 20 sets of coded conditions (composing a full replication with three factors of eight points, six corner points and six centre points) was chosen in this investigation.

Table 4 presents the ranges of factors considered, and Table 5 shows the 20 sets of coded and actual values used to conduct the experiments.

Table 4 Important factors and their levels

Factor	Level				
	−1.682	−1	0	+1	+1.682
pH value	3	4.62	7	9.38	11
Spraying time, t/h	24	40.20	64	87.80	104
Cl^- concentration, c/(mol·L^{-1})	0.2	0.36	0.6	0.84	1

For the convenience of recording and processing experimental data, the upper and lower levels of the factors were coded here as +1.682 and −1.682, respectively. The coded values of any intermediate value could be calculated using following relationship:

Table 5 Design matrix and experimental results

Experiment No.	pH	Spraying time, t/h	Cl^- concentration, c/(mol·L^{-1})	Mass loss, Δm/g	Corrosion rate, R_c/(mm·a^{-1})
1	4.62	40.00	0.36	0.1350	0.1462
2	9.38	40.20	0.36	0.0945	0.1023
3	4.62	87.80	0.36	0.2385	0.1189
4	9.38	87.80	0.36	0.1803	0.0899
5	4.62	40.20	0.84	0.1462	0.1582
6	9.38	40.20	0.84	0.1045	0.1131
7	4.62	87.80	0.84	0.2591	0.1292
8	9.38	87.80	0.84	0.2156	0.1075
9	3.00	64.00	0.60	0.2202	0.1496
10	11.00	64.00	0.60	0.2705	0.1838
11	7.00	24.00	0.60	0.0619	0.1123
12	7.00	104.00	0.60	0.2180	0.0912
13	7.00	64.00	0.20	0.1160	0.0790
14	7.00	64.00	1.00	0.1589	0.1080
15	7.00	64.00	0.60	0.1455	0.0989
16	7.00	64.00	0.60	0.1262	0.0856
17	7.00	64.00	0.60	0.1263	0.0858
18	7.00	64.00	0.60	0.1262	0.0857
19	7.00	64.00	0.60	0.1262	0.0857
20	7.00	64.00	0.60	0.1262	0.0856

$$X_i=1.682[2X-(X_{max}-X_{min})]/(X_{max}-X_{min}) \quad (1)$$

where X_i is the required coded value of a variable X; X_{min} is the lower level of the variable; X_{max} is the upper level of the variable.

2.4 Recording responses

The corrosion rate of the AA2024 aluminium alloy specimen was estimated by mass loss measurement under salt fog tests as per ASTM B−117. The original mass (m_0) of the specimen was recorded and then the specimen was sprayed with the solution of NaCl for different immersion time of 40.20, 64, 87.80 and 104 h. Finally, the corrosion products were removed by immersing the specimens for 5 to 10 min in a solution boiled at 90 °C prepared by using 50 mL phosphoric acid (H_3PO_4, specific gravity of 1.69 g/cm^3) and 20 g chromium trioxide (CrO_3) and reagent water to make 1000 mL. If corrosion product films remain, rinse, and then follow with nitric acid (HNO_3, density of 1.42 g/cm^3) for 1 to 5 min at 20 to 25 °C, the solution temperature was maintained at 25 °C using a thermostat. These specimens were washed with distilled water, dried and weighed again to obtain the final mass (m_1). The weight loss (Δm) could be measured using the following relation,

$$\Delta m=(m_0-m_1) \quad (2)$$

where Δm is the mass loss (g); m_0 is the original mass before test (g); m_1 is the final mass after test (g).

The corrosion rate of AA2024 aluminium alloy weld metal region could be calculated by using the following equation by conducting the immersion test as per ASTM standards G1-03:

$$R_c=\frac{8.7610^4\Delta m}{ADt} \quad (3)$$

where R_c is the corrosion rate (mm/a); A is the surface area of the specimen (cm^2); D is the density of the material (2.73 g/cm^3); τ is the corrosion time (h).

Microstructural analysis was carried on the corroded specimens using a light optical microscope (Union. Opt. Co. Ltd., Japan; VERSAMET−3) incorporated with an image analyzing software (Clemex-vision). The exposed specimen surface was prepared for the micro examination both in the "AS polished" and "AS etched" conditions. Picral acid and acetic acid were used as etchant. The corrosion test specimens were polished in disc polishing machine for fewer scratch surfaces and the surface was observed using optical microscope. Furthermore, the pitting characterization and the determination of corrosion products were done using SEM-EDS (Carl Zeiss, GmbH, Germany; EVO 50) attached with Bruker AXS Quantax 4010 Energy dispersive X-ray spectrometer (EDS).

3 Results and discussion

The corrosion rates of weld specimens in different concentrations of NaCl solutions with different pH values at different spraying time period were obtained and tabulated in the Table 5. In the salt fog tests, it was observed that the corrosion rate decreased as the pH increased to neutral. For every chloride ion concentration and spraying time, the weld metal usually exhibits a decrease in the corrosion rate with an increase in the pH value from acidic to neutral. At a neutral pH, the corrosion rate was faintly reduced, and a significantly high corrosion rate was observed in an alkaline solution.

3.1 Effect of pH value

Figure 4 shows the effect of pH on corrosion rate of AA2024 aluminium welds sprayed in 0.6 mol/L NaCl for 64 h with different pH values of 3, 7 and 11. The results from Fig. 5 demonstrated that, when the alloy is submitted to spraying in neutral pH media, a decrease is observed in the corrosion rate, and an increase is seen in this if the values of the pH are displaced in acidic or

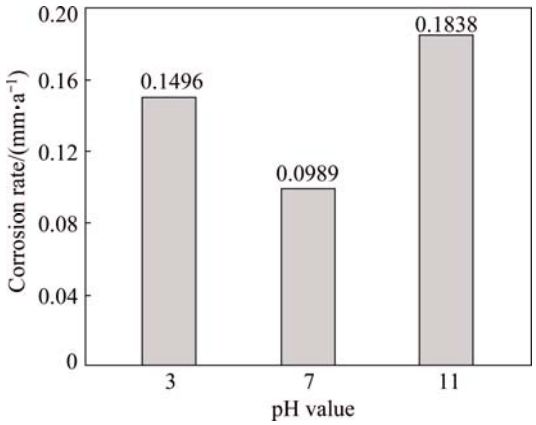

Fig. 4 Effect of pH value on corrosion rate of AA2024 aluminium welds sprayed in 0.6 mol/L NaCl for 64 h with different pH values

alkaline pH. In other words, there is an increase in the alloys susceptibility to corrosion in the acidic and purely alkaline media.

The results obtained above can be interpreted by considering the fact that the chemical reactions of aluminum and its alloys are unusual in the sense that these materials are amphoteric, i.e., soluble in acid as well as in alkali solutions [22,23]. In acidic solution, the solubility of Al^{3+} facilitates the dissolution of the Al matrix and further accelerates the chloride attack. However, the mechanism of corrosion of the Al matrix in neutral and alkaline media is related with the formation of protective layer of aluminum hydroxides $Al(OH)_3$.

The oxide film is uniformly thinned by the chemical dissolution, which is facilitated by the presence of high OH^- concentration in alkaline solution [24]. Whereas in neutral pH solutions, the passive film of aluminum hydroxides ($Al(OH)_3$) formed on AA2024 aluminium welds surface is remarkably stable due to its low solubility, acting as protector for this welds against corrosive agents.

Figure 5 shows the effect of pH on corrosion and pit morphologies of AA2024 aluminium welds sprayed in

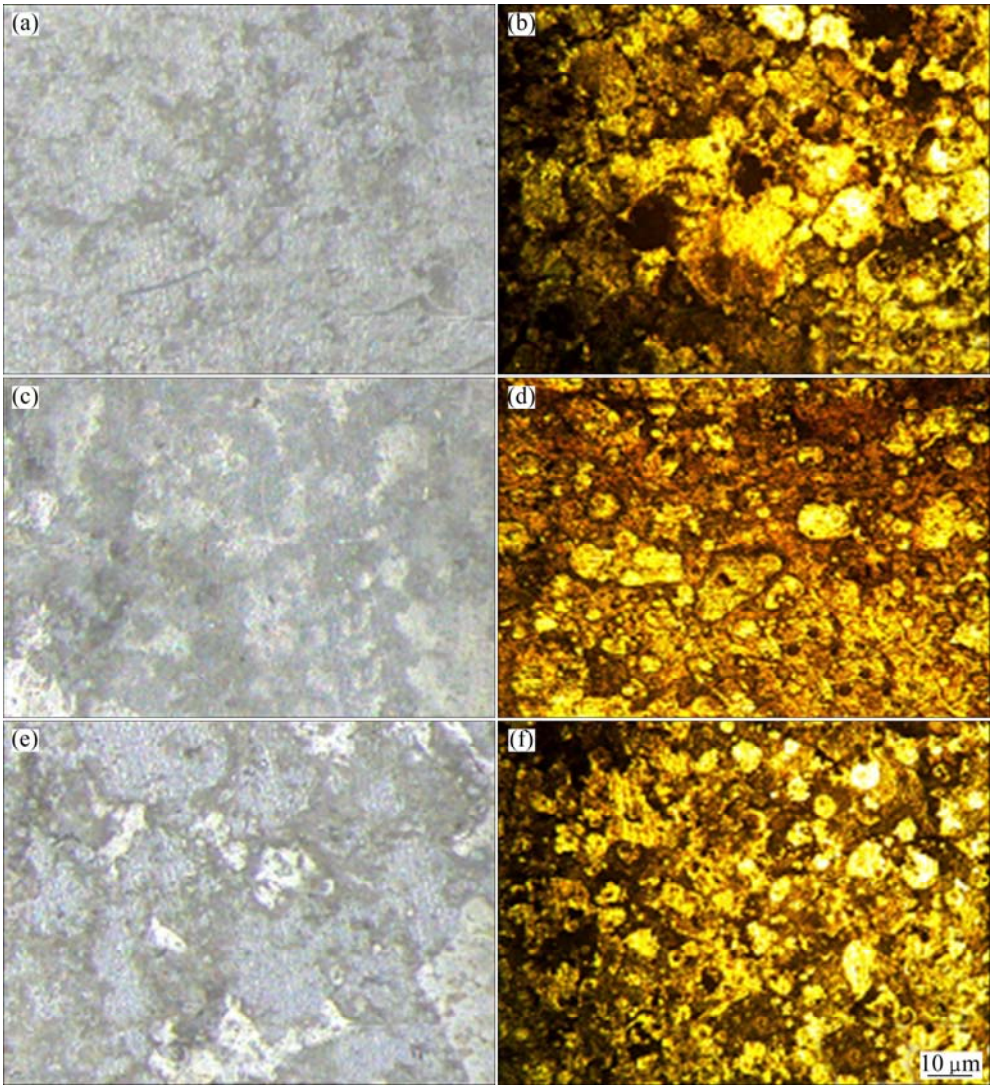

Fig. 5 Effect of pH value on corrosion morphologies (a, c, e) and pit morphologies (b, d, f) of AA2024 aluminium welds sprayed in 0.6 mol/L NaCl solution for 64 h: (a, b) pH=3; (c, d) pH=7; (e, f) pH=11

0.6 mol/L NaCl for 64 h with different pH values of 3, 7 and 11. It is found that the corrosion morphology of the welds shows more grooves. The surface of the specimen possesses more grooves in acidic solutions, and slightly corroded in neutral solutions. A sever attack with a greyish oxide layer has been seen in the specimens sprayed with alkaline solutions.

In these welds, evidence of cathodic reactivity is found in the form of grooves around constituent intermetallic particles. However, on the surface (corroded area) of weld region, some intergranular attacks are also observed. In all cases, the welds show grooves around intermetallic particles, which is more evident from the pit morphology. The grooves around the constituent particles are the consequence of the cathodic reduction of oxygen, which takes place at the constituent particles and causes an increase in alkalinity in the solution around the particles, leading to the dissolution of aluminium matrix [25].

The pit morphology clearly shows that hemispherical pits with different sizes were grown throughout the surfaces of the samples and around each pit a white corrosion product was accumulated as the result of the corrosion of the aluminum alloy matrix in the vicinity of the precipitates. Attack with similar morphology has been reported by other authors as localized alkaline corrosion [26]. These micrographs clearly show that the damage caused by this type of corrosion is accentuated in solutions of acidic pH compared to that in slightly neutral solution, suggesting that the anodic activity of the system became intense with this acid range of pH. Spraying to solution of alkaline pH resulted in more intense corrosion attack. As consequence of this treatment, a film of oxide is formed over the surface of the sample, which is covered with white gelatinous mass, normally called alumina.

It was also determined that the *S* phase occupied 2.7% of the total surface area. This phase was active and Mg and Al selectively dissolved, leaving a pit where the particle was present. The *S* phase dealloying left Cu-rich particle remnants, which were cathodic to the matrix and therefore caused the peripheral formation of pits around the particle. It is interesting to note that some of the Cu-rich particles decomposed into small mobile clusters and could be carried out from the pit probably by mechanical action which is clearly shown in the SEM analysis.

3.2 Effect of spraying time

Figure 6 shows the effect of spraying time on corrosion rate of AA2024 aluminium welds sprayed in NaCl solutions of pH 7 with chloride ion concentration of 0.6 mol/L at different spraying time of 24, 64 and 104 h. With the increase of corrosion time, the corrosion rate decreases for the specimens undergone salt spray corrosion tests. It is proved that the outer layer made a predominant role to strike against corrosion with the increase of time.

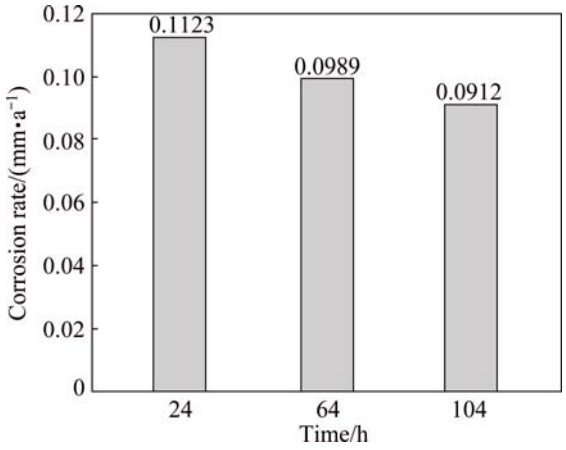

Fig. 6 Effect of spraying time on corrosion rate of AA2024 aluminium welds sprayed in NaCl solutions of pH 7 with chloride ion concentration of 0.6 mol/L at different spraying time

Figure 7 shows the effect of spraying time on corrosion and pit morphologies of AA2024 aluminium welds sprayed in NaCl solutions of pH 7 with chloride ion concentration of 0.6 mol/L. During the salt spray corrosion testing, dark patches were observed on the surface of the specimens with increasing spraying time. It results in an increase in hydrogen evolution with increasing spraying time, which tends to increase the concentration of OH^- ions, strengthening the surface from further corrosion [30]. It was also found that the increase in spraying time enhanced the tendency to form corrosion products, which accumulated over the surface of the samples. These corrosion products, in turn, depressed the corrosion rate due to the passivation in the salt foggy environment. However, with the increase of spraying time, the corrosion product formed is known to be $Al(OH)_3$. The EDS microanalysis of the corroded products was carried out. However, as this technique cannot reveal the presence of hydrogen, the presence of $Al(OH)_3$ could not be proved at the moment. Attempts are tried to carry in FTIR studies to prove the presence of $Al(OH)_3$ as a part of the future work.

From the pit morphology, the pits with very small diameter and deeper depth were observed on the surface after corrosion test and a continuous decrease in thickness over the entire surface area of the metal was observed throughout the corrosion test in the specimen exposed for 24 h. But later with the increment of time, the pits grow wider in the presence of corrosion products. To investigate the susceptibility to intergranular attack, no continuous secondary phase particle has been

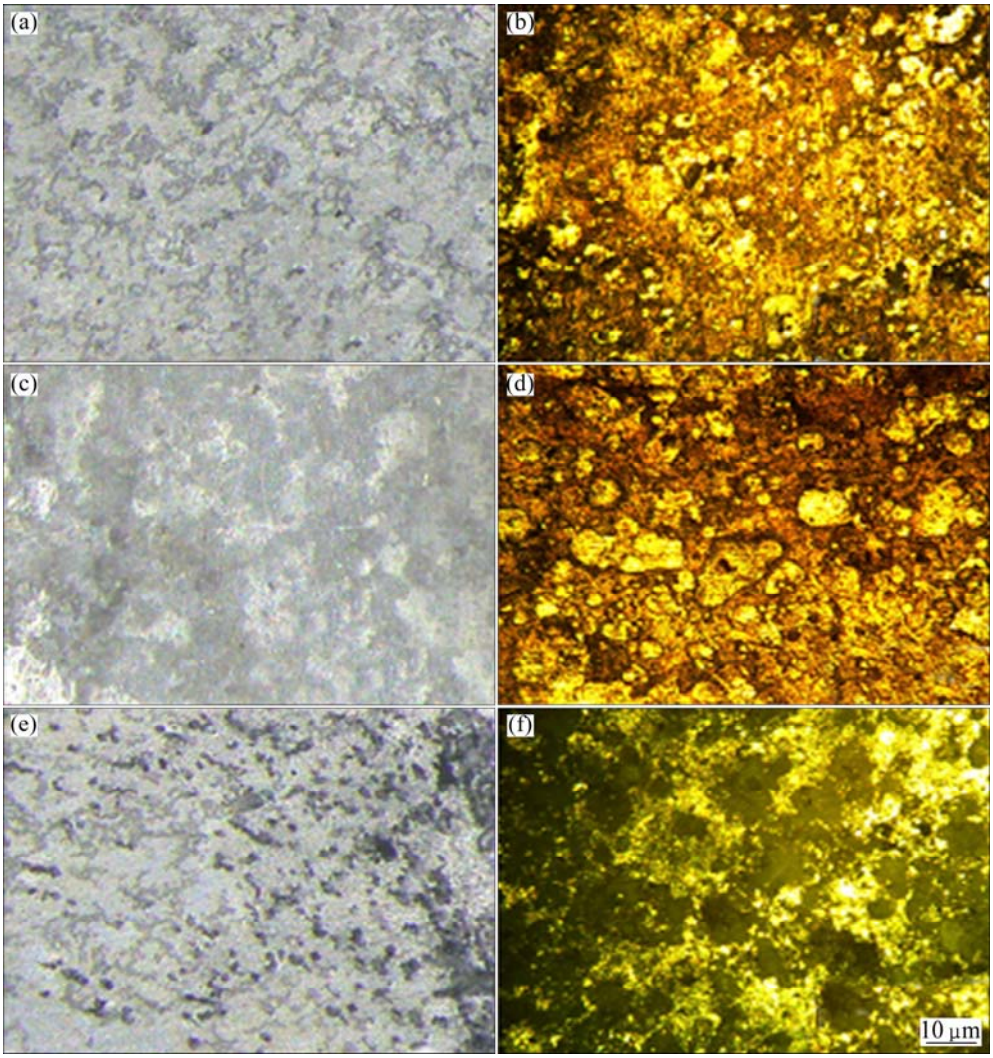

Fig. 7 Effect of spraying time on corrosion morphologies (a, c, e) and pit morphologies (b, d, f) of AA2024 aluminium welds sprayed in NaCl solutions of pH 7 with chloride ion concentration of 0.6 mol/L: (a, b) 24 h; (c, d) 64 h; (e, f) 104 h

observed. Only pits were observed from the pit morphology. The propagation of intergranular corrosion starts at pits. This indicates that it needs some more time for the intergranular cracks to propagate.

3.3 Effect of chloride ion concentration

Figure 8 shows the effect of chloride ion concentration on corrosion rate of AA2024 aluminium welds sprayed in NaCl solutions of pH 7 for 64 h. In the salt fog tests, it was observed that the corrosion rate increased as the chloride ion concentration increased. For every pH value and spraying time, the weld metal usually exhibited an increase in the corrosion rate with an increase in the chloride ion concentration.

Figure 9 shows the effect of chloride ion concentration on corrosion and pit morphologies of AA2024 aluminium welds sprayed in NaCl solutions of pH 7 for 64 h. It was observed from the corrosion morphology that, when more Cl^- in NaCl solution

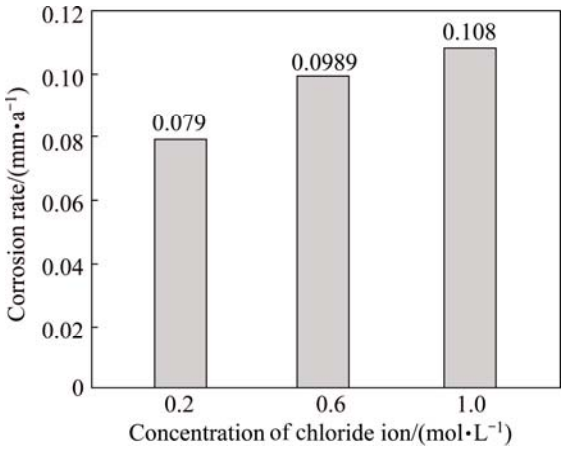

Fig. 8 Effect of chloride ion concentration on corrosion rate of AA2024 aluminium welds sprayed in NaCl solutions of pH 7 for 64 h

promoted the corrosion, the corrosive intermediate (Cl^-) would be rapidly transferred through the outer layer and

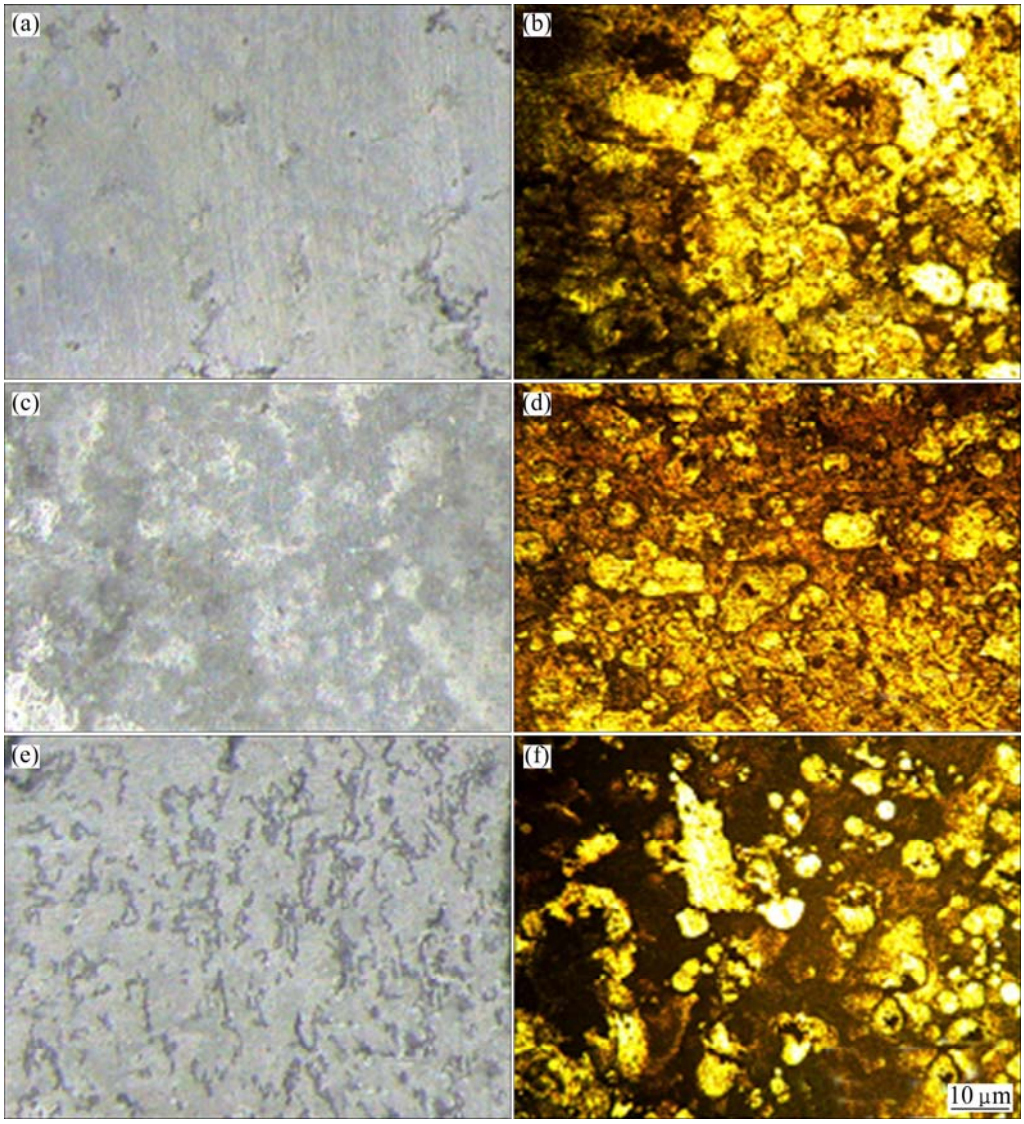

Fig. 9 Effect of chloride ion concentration on corrosion morphologies (a, c, e) and pit morphologies (b, d, f) of AA2024 aluminium welds sprayed in NaCl solutions of pH 7 for 64 h: (a, b) 0.2 mol/L; (c, d) 0.6 mol/L; (e, f) 1 mol/L

reached the substrate of the alloy surface. Hence, the corrosion rate was increased. But it was observed from the corrosion test results that the rising rate of corrosion with the increase of chloride ion concentration was reduced throughout the tests. This is due to the fact that within Al pits, the salt layer exists, if not during pit nucleation and the first stadium of pit growth, then during a later period of pit growth. As noted that on metals such as Mg, Zn, Al, Fe, Ni and Zr (i.e., metals that suffer pitting), the dissolution product $MeCl_x$ forms a solid salt in pits. It is almost unanimously accepted that a salt film stabilizes the pit. However, there is no clear knowledge on the composition of the salt layer. In the literature, two different types of pits salt are mentioned: aluminum chloride ($AlCl_3$) and aluminum oxychlorides $Al(OH)_2Cl$ and $Al(OH)Cl_2$. Depending upon the kind of a salt, different pH values of the solution within the pit can be expected. In the presence of $AlCl_3$, the pH should be as low as 4 [27]. On the other hand, the saturated solution of $Al(OH)_2Cl$ exhibits in neutral solutions, which slows down the corrosion rate [28]. According to the literature, the following sequence of reactions occurs, ionization of the bare surface of Al occurs rapidly and Al^{3+} undergoes hydrolysis very rapidly [29]. From the pit morphology, it was observed that the pitting was observed on the metal surface. The pits are more aggressive at higher chloride ion concentrations. The metal surface was found to be inhomogeneous, consisting of a number of defects, and the adsorption energy varied from site to site. Accordingly, the adsorption of chloride ions was determined to be local. It was concluded that a corroding aluminum surface has a variety of adsorption sites with different adsorption properties; only a minority of these sites are active for pitting corrosion.

According to the observations, the results suggest

that there is no threshold for the chloride concentration below which pitting will not occur.

3.4 Empirical relationship

In the present investigation, to correlate the salt fog test parameters and the corrosion rate of AA2024 aluminium welds, a second order quadratic model was developed. The response (corrosion rate) is a function of pH value (P), spraying time (t) and chloride ion concentration (c) and it can be expressed as

$$R_c=f(P,\ t,\ c) \tag{4}$$

The empirical relationship must include the main and interaction effects of all factors and hence the selected polynomial is expressed as follows:

$$Y=b_0+\sum b_i x_i+\sum b_{ii} x_i^2+\sum b_{ij} x_i x_j \tag{5}$$

For three factors, the selected polynomial can be expressed as

$$R_c=b_0+b_1(P)+b_2(t)+b_3(c)+b_{11}(P^2)+b_{22}(t^2)+b_{33}(c^2)+ b_{12}(Pt)+b_{13}(Pc)+b_{23}(tc) \tag{6}$$

where b_0 is the average of responses (corrosion rate) and b_1, b_2, b_3, ⋯, b_{11}, b_{12}, b_{13}, ⋯, b_{22}, b_{23}, b_{33}, are the coefficients that depend on the respective main and interaction factors, which are calculated using the expression given below:

$$B_i=\sum(X_i,\ Y_i)/n \tag{7}$$

where i varies from 1 to n, X_i is the corresponding coded value of a factor and Y_i is the corresponding response output value (corrosion rate) obtained from the experiment and n is the total number of combination considered. All the coefficients were obtained applying central composite rotatable design matrix using the Design Expert statistical software package. After determining the significant coefficients (at 95% confidence level), the final relationship was developed including only these coefficients. The final empirical relationship obtained by the above procedure to estimate the corrosion rate of friction stir welds of AA2024 aluminium alloy is given below:

$$R_c=0.095-0.015P-0.00804t+0.00940c+0.020P^2+ 0.00994c^2 \tag{8}$$

The analysis of variance (ANOVA) technique was used to find the significant main and interaction factors. The results of second order response surface model fitting as analysis of variance (ANOVA) are given in Table 6.

The determination coefficient (r^2) indicates the goodness of fit for the model. The model F-value of 15.04 infers that the model is significant. There was only a 0.01% chance that a "model F-value" this large could occur due to noise. Values of "Prob>F" less than 0.0500 indicate that model terms are significant. In this case, P, t, c, P^2 and c^2 are significant model terms. Values greater than 0.1000 indicate that the model terms are not significant. If there are many insignificant model terms (not counting those required to support hierarchy), model reduction may improve the model. The "lack of fit F-value" of 1.69 implies that the lack of fit is not significant relative to the pure error. There is a 6.20% chance that a "lack of fit F-value" this large could occur due to noise. Non-significant lack of fit is good. All these indicated an excellent suitability of the regression model. The observed values were compared with the experimental values, as shown in Fig. 10.

Table 6 ANOVA tests results

Source	Sum of squares	df	Mean square	F value	p-value	Model significance
Model	0.012	9	0.00139	15.04	0.0001	Significant
pH value, P	0.00318	1	0.00318	34.53	0.0002	
Spraying time, t	0.00088	1	0.00088	9.59	0.0113	
Chloride ion concentration, c	0.00121	1	0.00121	13.12	0.0047	
Pt	0.00019	1	0.00019	1.99	0.1884	
Pc	0.000004	1	0.000004	0.051	0.8266	
tc	0.000003	1	0.000003	0.035	0.8547	
P^2	0.00598	1	0.00598	64.97	< 0.0001	
t^2	0.00454	1	0.00454	0.00049	0.9827	
c^2	0.00142	1	0.00142	15.47	0.0028	
Residual	0.00092	10	0.00092			
Lack of fit	0.00075	5	0.00015	4.51	0.0620	Not significant
Pure error	0.00016	5	0.000033			
Correlation total	0.013	19				

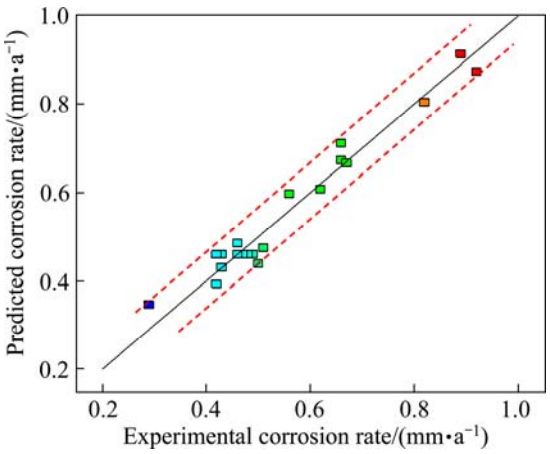

Fig. 10 Correlation graph for response (Salt spray corrosion test)

3.5 SEM analysis

The pitting corrosion occurred in every region after being sprayed in NaCl solutions for 24 and 104 h with the chloride ion concentration of 0.6 mol/L and pH 7, as shown in Fig. 11. The initial galvanic couple of pitting corrosion was found in the region between the *S* phase particles and their adjacent aluminium matrix. The *S* phase particles as anode took priority in dissolving due to the lower self-corrosion potential compared to the adjacent aluminium matrix. With increasing spraying time, the *S* phase particles became smaller and smaller, which means that the elements Al and Mg in the *S* phase were dissolved continuously during the initial stage. With decreasing contents of Al and Mg elements in the *S* phase, the change in the distribution of Cu element from the edge to the center in the particle resulted in the raising of the self-corrosion potential of the *S* phase. Consequently, the *S* phase conversely acted as the cathode and led to the anodic dissolution of the adjacent aluminium matrix. Also, it was noted from the EDS that peaks of chloride and natrium were observed. This reveals more attacks of the aluminium alloy welds since they are exposed to NaCl solutions.

However, after 24 h, the samples then presented signs of localized attack. This behaviour is similar to that described for alloy AA2024-T4 [31]. It shows the appearance of these intermetallics after the spraying in a solution of NaCl for 104 h. The presence of higher peaks of oxygen in the EDS and the fact that their composition hardly varies, together with the type of corrosion displayed in the neighbouring aluminium matrix, tend to confirm the cathodic characteristics of these intermetallics. Thus, the process of reduction of O_2 to OH^- takes place on these intermetallics, and the oxidation of the matrix is the associated anodic response. The local increase of the pH is the factor responsible for the dissolution of the layer and matrix in proximity to these intermetallics. The copper originates from the Al(Cu,Mg) intermetallics themselves; once, the Al and Mg in these particles have been desalted, the remaining Cu gets dissolved due to its porous structure. The copper

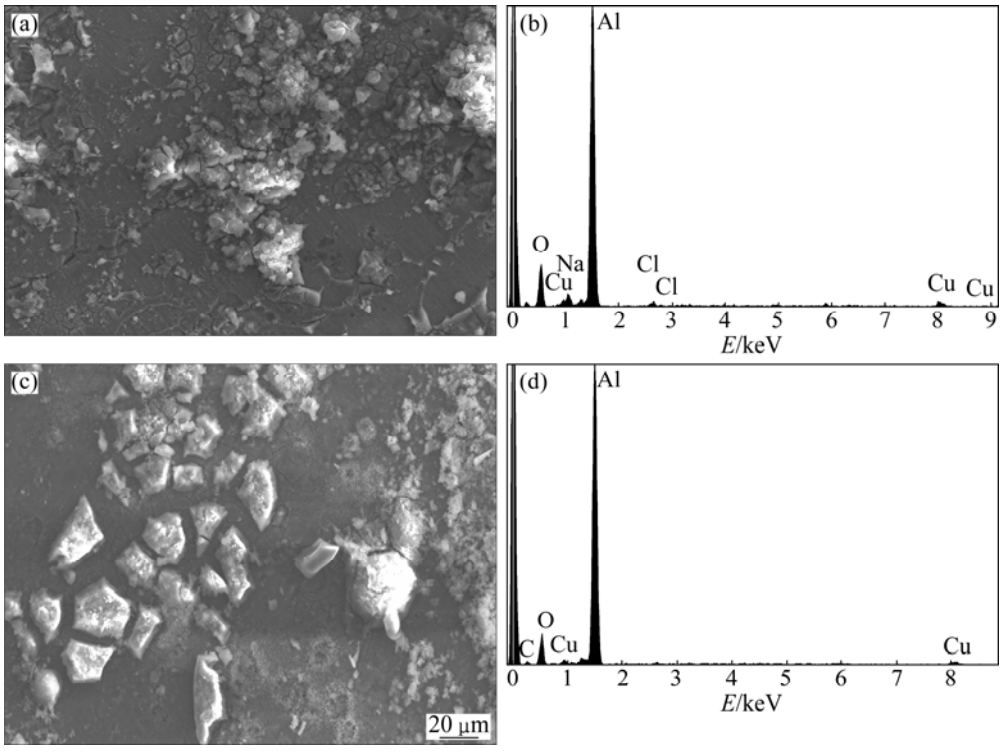

Fig. 11 SEM images and EDS analysis of AA2024 weld specimens after corrosion in NaCl solutions with pH 7 and chloride ion concentration of 0.6 mol/L: (a, b) Spraying time of 24 h; (c, d) Spraying time of 104 h

in solution is then reduced on the points of cathodic characteristics with the increment of spraying time, such as the Al intermetallics, and appears in the form of small nodules.

4 Conclusions

1) The corrosion rate decreases with the increase of pH value from acidic to neutral. Further increase of corrosion rate is seen from neutral to alkaline. This is due to the instability of aluminium oxide layer in acidic and alkaline solutions.

2) With the increase in the chloride ion concentration, the corrosion rate increases in the salt spray corrosion test. But the rising rate of corrosion decreases due to the formation hydroxyl chloride layer.

3) The corrosion rate decreases with the increase of spraying time, but the corrosion tends to be uniform with the increment of time.

4) On microstructural examination, it is proved that the corrosion morphology and pit morphology of the FSW AA2024 welds depend mainly on the pH value of the solution, the spraying time and the chloride ion concentrations. In the FSW welds, the *S* phases, i.e., secondary phases, act cathodic to α(Al) matrix, which accelerate the corrosion.

References

[1] MATRUKANITZ R P. Selection and weldability of heat-treatable aluminum alloys [M]//ASM Handbook-Welding, Brazing and Soldering. Metals Park, OH: ASM International, 1999.

[2] THOMAS W M, NICHOLAS E D, NEEDHAM J C, MURCH M G, SMITH P T, DAWES C J. Friction stir butt welding: International Patent, PCT/GB92/02203 [P]. 1991−12−18.

[3] THOMAS W M, NICHOLAS E D. Friction stir welding for the transportation industries [J]. Materials and Design, 1997, 18: 269−273.

[4] ERICSSON M, SANDSTROM R. Influence of welding speed on the fatigue of friction stir welds, and comparison with MIG and TIG [J]. International Journal of Fatigue, 2003, 25: 1379−1387.

[5] BALASUBRAMANIAN V, LAKSHMINARAYANAN A K. The mechanical properties of the GMAW, GTAW and FSW joints of the RDE-40 aluminium alloy [J]. International Journal of Microstructure and Materials Properties, 2008, 3: 837−853.

[6] XU W F, LIU J H, LUAN G H, DONG C L. Microstructure and mechanical properties of friction stir welded joints of aluminum alloy thick plate with different welding state [J]. Acta Metallurgica Sinica, 2009, 45: 490−496.

[7] ELANGOVAN K, BALASUBRAMANIAN V, VALLIAPPAN M. Influences of pin profile and rotational speed of the tool on the formation of friction stir processing zone in AA2219 aluminium alloy [J] Journal of Materials Science Engineering A, 2007, 459: 7−18.

[8] RAJAKUMAR S, MURALIDHARAN C, BALASUBRAMANIAN V. Establishing empirical relationships to predict grain size and tensile strength of friction stir welded AA 6061-T6 aluminium alloy joints [J]. Transactions of Nonferrous Metals Society of China, 2010, 20: 1863−1872.

[9] DÍAZ-BALLOTE L, LÓPEZ-SANSORES J F, MALDONADO-LÓPEZ L, GARFIAS-MESIAS L F. Corrosion behaviour of aluminium exposed to a biodiesel [J]. Electrochemistry Communications, 2009, 11: 41−44.

[10] XU W F, LIU J H. Microstructure and pitting corrosion of friction stir welded joints in 2219-O aluminum alloy thick plate [J]. Corrosion Science, 2009, 51: 2743−2751.

[11] WADESON D A, ZHOU X, THOMPSON G E, SKELDON P, DJAPIC O, SCAMANS G. Corrosion behaviour of friction stir welded AA7108 T79 aluminium alloy [J]. Corrosion Science, 2006, 48: 887−897.

[12] JARIYABOON M, DAVENPORT A J, AMBAT R, CONNOLLY B J, WILLIAMS S W, PRICE D A. The effect of welding parameters on the corrosion behaviour of friction stir welded AA2024–T351 [J]. Corrosion Science, 2007, 49: 877−909.

[13] AMIN M A, ABD EI-REHIM S S, EL SHERBINI E E F, HAZZAZI O A, ABBAS M N. Polyacrylic acid as a corrosion inhibitor for aluminium in weakly alkaline solutions. Part I: Weight loss, polarization, impedance EFM and EDX studies [J]. Corrosion Science, 2009, 51: 658−667.

[14] XU W F, LIU J H, LUAN G H AND DONG C L. Temperature evolution, microstructure and mechanical properties of friction stir welded thick 2219-O aluminum alloy joints [J]. Materials & Design, 2009, 30: 1886−1893.

[15] CONNOLLY B J, DAVENPORT A J, JARIYABOON M, PADOVANI C, AMBAT R, WILLIAMS S W, PRICE D A. Friction stir welding of aluminium alloys [C]//Proceedings of 5th International Friction Stir Welding Symposium. Metz: France, 2004: 15−24.

[16] WILLIAMS S, AMBAT R, PRICE D, JARIYABOON M, DAVENPORT A, WESCOTT A. Laser treatment method for improving of the corrosion resistance of friction stir welds [J]. Material Science Forum, 2003, 426: 2855−2860.

[17] CORRAL J, TRILLO E A, LI Y, MURR L E. Corrosion of friction-stir welded aluminum alloys 2024 and 2195 [J]. Material Science Letters, 2000, 19: 2117−2122.

[18] DELTOMBE E, POURBAIX M. The electrochemical behavior of aluminum: Potential pH diagram of the system Al−H_2 at 25 °C [J]. Corrosion, 1953, 14: 496−500.

[19] BROWN O R, WHITLEY J S. Electrochemical behaviour of aluminium in aqueous caustic solutions [J]. Electrochimica Acta, 1987, 32: 545−556.

[20] MOON S M, PYUN S I. The corrosion of pure aluminium during cathodic polarization in aqueous solutions [J]. Corrosion Science, 1997, 39: 399−408.

[21] PYUN S I, MOON S M, AHN S H, KIM S H. Effects of Cl^-, NO^-_3 and SO_4^{2-} ions on anodic dissolution of pure aluminum in alkaline solution [J]. Corrosion Science, 1999, 41: 653−667.

[22] HOLLINGSWORTH E H, HUNSICKER H Y [M]//ASM Handbook of Corrosion. (Vol. 13). Metals Park, OH: ASM International, 1992.

[23] ZAID B, SAIDI D, BENZAID A, HADJI S. Effects of pH and chloride concentration on pitting corrosion of AA6061 aluminum alloy [J]. Corrosion Science, 2008, 50: 1841−1847.

[24] ABALLE A, BETHENCOURT M, BOTANA F J, CANO M J, MARCOS M. Localized alkaline corrosion of alloy AA5083 in neutral 3.5% NaCl solution [J]. Corrosion Science, 2001, 43: 1657−1674.

[25] SEHGAL A, LU D, FRANKEL G S. Pitting in aluminum thin films: Super saturation and effects of dichromate ions [J]. Journal of Electrochemical Society, 1998, 145: 2834−2840.

[26] VIJH A K. The pitting potentials of metals: The case of titanium [J]. Corrosion Science, 1973, 13: 805−806.

[27] BOAG A, HUGHES A E, GLENN A M, MUSTER T H, MCCULLOCH D. Corrosion of AA2024-T3. Part I: Localised

corrosion of isolated IM particles [J]. Corrosion Science, 2011, 53: 17−26.

[28] SUREKHA K, MURTY B S, PRASAD RAO K. Microstructural characterization and corrosion behavior of multipass friction stir processed AA2219 aluminium alloy [J]. Surface & Coatings Technology, 2008, 202: 4057−4068.

[29] BUCHHEIT R G, GRANT R P, HLAVA P F, MCKENZIE B, ZENDER G L. Local dissolution phenomena associated with *S* phase (Al_2CuMg) particles in aluminum alloy 2024-T3 [J]. Journal of the Electrochemical Society, 1997, 144: 2621−2628.

[30] GUILLAUMIN V, MANKOWSKI G. Localized corrosion of 2024 T351 aluminum alloy in chloride media [J]. Corrosion Science, 1999, 41: 421−438.

[31] QUEIROZ F M, MAGNANI M, COSTA I, DE MELO H G. Investigation of the corrosion behaviour of AA2024-T3 in low concentrated chloride media [J]. Corrosion Science, 2008, 50: 2646−2657.

摩擦搅拌焊 AA2024 铝合金在盐雾条件下的腐蚀性能

R. SEETHARAMAN[1], V. RAVISANKAR[1], V. BALASUBRAMANIAN[2]

1. Department of Manufacturing Engineering, Annamalai University, Annamalainagar, Chidambaram 608 002, Tamil nadu, India;
2. Center for Materials Joining & Research, Department of Manufacturing Engineering, Annamalai University, Annamalainagar, Chidambaram 608 002, Tamil nadu, India

摘　要：2024 铝合金是一种重要的工程材料，被大量应用于航空工业。但是在含氯介质中，2024 铝合金易于腐蚀。本研究对 5 mm 厚 AA2024 铝合金轧板进行摩擦搅拌焊接。通过 NaCl 溶液盐雾腐蚀试验对试样在不同 pH 值、氯离子浓度和喷雾时间条件下的腐蚀性能进行评价。建立一个经验关系式对摩擦搅拌焊 AA2024 铝合金的腐蚀速率进行预测。采用含有 3 因素 5 水平的中心复合旋转设计以减少实验次数。采用响应曲面法研究实验参数间的关联关系。在中性 pH 条件下，腐蚀速率降低；而在碱性和酸性条件下，腐蚀速率增加。随着喷雾时间的增加，腐蚀速率降低，但腐蚀趋于均匀，而随着氯离子浓度的增加，腐蚀速率增加。

关键词：AA2024 铝合金；摩擦搅拌焊；盐雾实验；响应曲面法；腐蚀速率

(Edited by Yun-bin HE)